Scintillation properties of the $YVO_4:Eu^{3+}$ compound in powder form: its application to dosimetry in radiation fields produced by pulsed mega-voltage photon beams

Nahuel Martinez[1], **Tobias Teichmann**[2], **Pablo Molina**[1], **Marian Sommer**[2], **Martin Santiago**[1], **Jürgen Henniger**[2], **Eduardo Caselli**[1,*]

[1] Instituto de Física Arroyo Seco - CIFICEN (CONICET – UNCPBA), Pinto 399, 7000 Tandil, Argentina
[2] Dresden University of Technology, Institute of Nuclear and Particle Physics, Radiation Physics Group, D- 01062 Dresden, Germany

Received 4 November 2014; accepted 4 April 2015

Abstract

The investigation of scintillation properties of europium doped yttrium orthovanadate shows the suitability of this material for fiber-based dose rate measurements. All measurements were carried out with a 6 MV Varian linear accelerator. The temperature dependence of the signal is lower than that of the plastic scintillators reported so far. By measuring the afterglow of probes between Linac-pulses, the signal due to the stem effect can be successfully eliminated. Comparison of depth dose profiles in a water phantom for radiation field dimensions between 1 x 1 cm^2 and 10 x 10 cm^2 shows that the probes are suitable for small fields having dimensions up to 1 x 1 cm^2. The high light yield of probes having dimensions of 1 mm opens up the possibility for their use in spatially confined radiation fields, such as in intensity-modulated radiotherapy (IMRT) and volume-modulated radiation therapy (VMAT).

Keywords: Scintillator detector, fiber-based dose rate measurements, radiotherapy

Szintillationseigenschaften der YVO4:Eu^{3+}-Verbindung in Pulverform: ihre Anwendung auf die Dosimetrie in den durch gepulste Megavolt-Photonenstrahlen erzeugten Strahlungsfeldern

Zusammenfassung

Die Untersuchung der Szintillationseigenschaften von europiumdotiertem Yttrium-Orthovanadat zeigt die Eignung dieses Materials für faserbasierte Dosisleistungsmessungen. Alle Messungen wurden an einem 6-MV-Linearbeschleuniger der Firma Varian durchgeführt. Die Temperaturabhängigkeit des Signals ist geringer als die von handelsüblichen Plastikszintillatoren. Durch die Messung des Nachleuchtens des Szintillationsprozesses können die Signalanteile von Cherenkov-Strahlung und Faserlumineszenz erfolgreich eliminiert werden. Der Vergleich von Tiefendosisprofilen in Wasserphantomen für Strahlungsfeldabmessungen zwischen 1 x 1 cm^2 und 10 x 10 cm^2 empfehlen die Anwendung der untersuchten Sonden für kleine Feldabmessungen im Bereich von 1 x 1 cm^2. Dies eröffnet Möglichkeiten für die Anwendung in räumlich stark begrenzten Strahlungsfeldern, wie sie bei intensitätsmodulierter Radiotherapie (IMRT) und volumenmodulierter Strahlentherapie (VMAT) zum Einsatz kommen.

Schlüsselwörter: Szintillationdetektor, faserbasierte Dosisleistungsmessungen, Röntgentherapie

* Corresponding author: Dr. Eduardo Caselli, Universidad Nacional del Centro Physics, Pinto 399, 7000 Tandil, Buenos Aires, Argentina.
E-mail addresses: ecaselli@exa.unicen.edu.ar, caselli44@gmail.com (E. Caselli).

Introduction

Scintillator detectors have been introduced by S. Curran and W. Baker in 1944 [1,2]. They employed ZnS, a material used by W. Crooks to construct in 1903 a screen to observe radioactive emissions. Since then many types of scintillating inorganic and organic substances have been investigated in order to construct detectors for different applications in research, industry and medicine. In particular, the advent of new technologies in radiotherapy, such as intensity modulated radiation therapy (IMRT) and volumetric modulated arc therapy (VMAT), which are characterized by the superimposition of small fields, in-vivo and real time dosimetry permits the detection of errors and differences between planned and delivered dose. In particular measurements of out-of-field doses are advisable since planning systems are not accurate outside the radiation beam [3]. In 1964 a scintillating plastic has been employed for the first time for dose measurements [4]. Later, plastic scintillators (PS) have been attached to an optical fiber in order to transport the light to a phototube outside the treatment room [5–7]. This technique is known as fiber optic dosimetry (FOD). Much attention has been focused on PS because these materials are near-tissue equivalent regarding their interaction with electrons, X- and γ-radiation, and feature dose linearity and resistance to radiation damage [5–7]. PS has a drawback common to all scintillators, namely, the dependence of the signal on temperature [7–11].

Inorganic scintillators have been also investigated for FOD. Al_2O_3:C is a near-tissue-equivalent compound. Since the output depends on dose, it has to be employed in saturation mode [12]. BeO is also near tissue-equivalent, and a promising material [13]. Its scintillation output is an order of magnitude lower than that of Al_2O_3:C [13].

The scintillation, also called radioluminescence (RL), of some non tissue-equivalent scintillators has been investigated: Ruby [14,15], GaN [16], and Y_2O_2S: Eu, YVO_4:Eu and Y_2O_3:Eu scintillators [17,18]. Recently Yb3+-doped silica fibers have been investigated for real time ionizing radiation detection [19].

Unlike detectors having an effective Z, denoted with Z_{eff}, close to that of water, the dose to a detector having a higher Z_{eff} over the dose to water will change with photon energy [20]. For mega-voltage energies the relationship exhibits relative low energy dependence, while the dependence is strong for energies, for which the photoelectric effect dominates. Thus for dose deposition in non tissue equivalent materials there is a deviation to the dose to water, which depends on the energy spectrum of the photons.

For mega-voltage beams low energy photons result from multiple Compton scattering. Therefore the percentage of low energy photons increases as the dimension of a beam increases. This has as consequence that the difference between the signal of a detector having a high Z_{eff} and an ionization chamber becomes larger as the dimension of a beam increases. Thus, in order to use a detector for mega-voltage beams the low energy photons should be eliminated. This is the reason why commercially available diodes for radiotherapy are sold with shielding caps [21].

A problem common to all FOD detectors is the light emitted by a fiber irradiated with high energy photons or/and electrons (stem effect). In the case of polymethyl methacrylate fibers (PMMA), for energies higher than 178 keV the stem effect is the sum of Cerenkov and fluorescence light. Several techniques have been proposed to reduce or eliminate the stem effect. The simplest one consists in placing a fiber with a scintillator side-by-side on a reference fiber without a detector. Thus the signal of the scintillator is obtained by subtracting the signal of the reference fiber from the signal of the fiber having the scintillator [5,22]. Another technique resorts to a fiber with a hollow air core [23]. A third method relies on the spectral discrimination to separate the scintillator signal from the stem effect [16,24,25]. A comparison of the three methods can be found in Ref. [26]. A fourth method consists in choosing luminescent ions that emit in the infrared region free from the spectral superposition of the stem effect [19]. Thus an increase in the stem radiation will not affect the RL emission. Finally the temporal discrimination of the RL signal from the stem emission should be mentioned. It consists in the measurement of the RL signal between pulses of a Linac [10,12,14,15,27,28]. This technique requires that the scintillator has an afterglow longer than the afterglow of the fiber, and we will refer to it as the Time Discrimination Filter (TDF). To the best of our knowledge this technique has been employed for the first time by Jordan [14]. He carried out measurements with a ruby crystal. The ^2E-$^4A_2$ transition of ruby at 694 nm has a lifetime of 3 ms, much longer than the lifetime of the stem effect, which for PMMA fiber is less than 5 μs [29]. Andersen et al. have employed Al_2O_3:C crystals having a signal decay characterized by two lifetimes: 35 and 178 ms [12]. When the afterglow is longer than the time between two successive pulses of a Linac, a saturation signal is reached for a time less than 1 second. As shown in reference 15, the saturation signal is a measure of the dose rate

Clift et al. employed a Bicron BC-444G detector, the afterglow of which lasts approximately 1200 ns [27]. Since the stem effect of the polystyrene fiber enclosed in polimethylmethacrylate cladding lasts nearly 700 ns, there is an overlap of the afterglow of the probe and the stem signal. Thus, by measuring the signal for t> 700 ns the stem effect is eliminated.

Detail information in the current status of scintillation dosimetry for megavoltage beams can be found in Ref. [30].

The aim of the investigations reported in this article was to characterize the RL of the YVO_4:Eu^{3+} compound in powder form to assess whether it is appropriate for dosimetry of megavoltage beams when the TDF is employed. The advantage of the TDF relies on the complete elimination of the stem effect if the afterglow of the fiber is negligible against the afterglow

of the probe. The characterization has been carried out by performing percentage depth dose measurements (PDD), and by measuring the signal dependence on temperature.

Material and detector

The $YVO_4:Eu^{3+}$ compound in powder form was produced by Phosphor Technology Ltd, England. The median particle size amounts to 6 μm. Its specific density amounts to 4.22 gr/cm^3, and its Z_{eff} is 25.4.

Twelve meters of a standard Super Eska PMMA optical fiber having a core diameter of 980 μm was used to guide the light from the sample to the photomultiplier tube. Nearly 2 mg powder was glued to one end of the fiber by employing the adhesive Norland 61.

The probe tip is encapsulated in light tight epoxy paint. Figure 1 shows the detector. The diameter of the encapsulated probe is 2.3 mm. The active part of the detector is a thin layer of powder attached to the surface of a fiber having a diameter lesser than 1 mm, and has a volume of nearly 0.5 mm^3 as computed from both the weight (2 mg) and the specific density. X-rays pictures taken with a digital mammography x-ray equipment (main energy 20 kev, resolution 35 μm) do not show clustering of the particles, at least clusters having dimension larger than 35 μm.

PMMA fibers have an attenuation coefficient of 0.3 dB/m for the wavelength of the strongest line of $YVO_4:Eu^{3+}$ compounds (λ=611 nm) [31]. Thus nearly 43% of the light entering at one end of a fiber will exit at the other end.

The light emitted by the probes has been recorded with a P25PC photon counting head module (SENS-TECH Ltd, UK) for performing percentage depth dose measurements, as reported below.

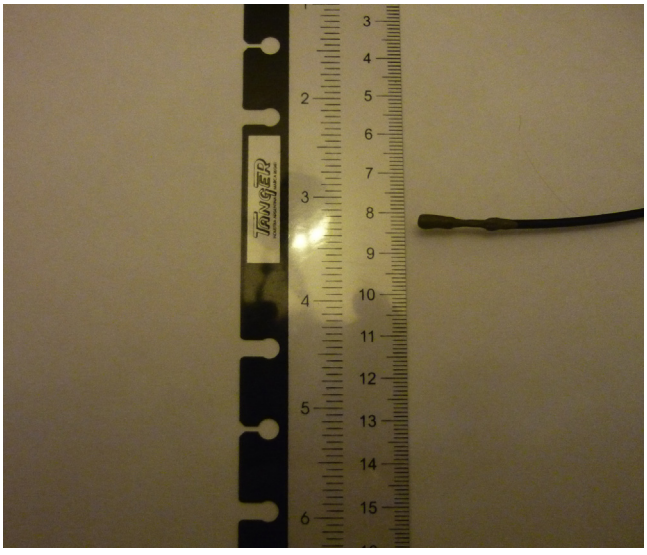

Figure 1. Detector for fiber optics dosimetry.

A Hamamatsu H7421-50 photon counting head was employed to determine the lowest detectable dose rate, and to compare the signal of the YVO_4:Eu powder with the signal delivered by a rod of Al_2O_3:Cr.

Time discrimination filter

In order to separate the stem effect contribution from the RL signal the time discrimination method was employed. A LabVIEW-controlled National Instruments USB-6251 card recorded the TTL pulses provided by P25PC photon counting head module (integration time 10 us). The measured signals were digitally recorded and processed in real time in order to integrate the TTL pulses only between the pulses produced by a Varian Linac 6MeV. The number of counts contained in the time interval between 50 μs after the beginning of a Linac pulse and 2000 μs are computed in real time, and the number of counts is taken as a measure of the dose rate.

Measurements

Percentage depth dose measurements (PDD) were carried out with a motorized water phantom (583 mm (L), 489 mm (W), 470 mm (D)). The scan velocity amounted to 3.76 mm/s. The source –water surface distance was 100 cm. The PDD measurements were also carried out with a pinpoint PTW chamber having a volume of 0.015 cm^3 and a diameter of 2 mm. The chamber was connected to a PTW UNIDOS-E electrometer.

For these measurements the P25PC photon counting head module was used.

Both the FOD detector and the chamber were placed perpendicular to the radiation beam.

A sketch of the set up is shown in Figure 2.

Results

Figure 3 shows the signals generated by a blank fiber. The large signals are produced by the Linac pulses, while the small pulses are noise. The afterglow of the fiber cannot be seen because the afterglow of the PMMA fiber lasts less than 5 μs, and the time resolution of the acquisition card amounts to 10 μs.

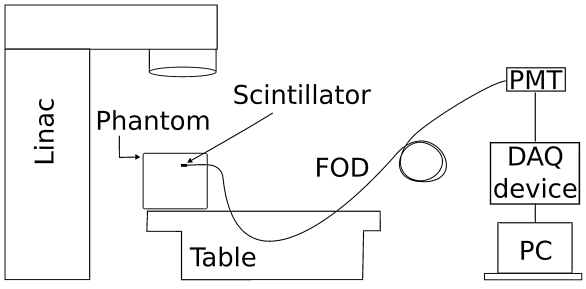

Figure 2. Experimental set-up.

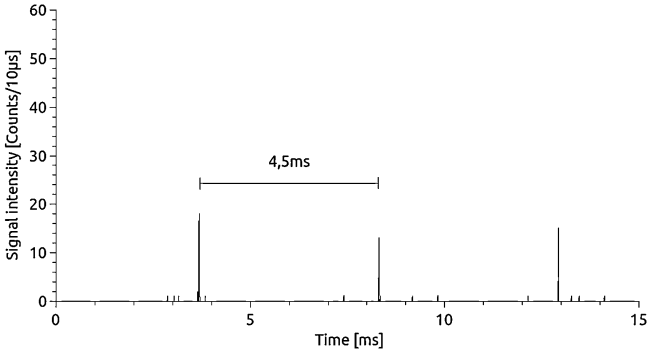

Figure 3. Signals from a blank fiber.

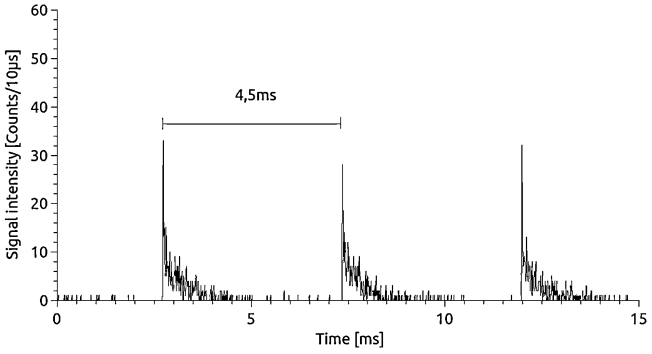

Figure 4. Signals delivered by a fiber with scintillator.

Figure 4 shows the signal delivered by a fiber with a YVO_4:Eu^{3+} probe. As stated above, the time between two consecutive pulses delivered by the Linac is 4.5 ms. The RL pulse lasts nearly 2.8 ms. The number of counts contained in the time interval between 50 μs after the beginning of a Linac pulse and 2000 μs are computed in real time, and the number of counts is taken as a measure of the dose rate. By doing so the stem is completed suppressed.

PDD measurements have been carried out for windows having dimensions between 1 cm x1 cm and 10 cm x 10 cm. For a window of 3 cm x 3 cm Figure 5 shows the signal of the

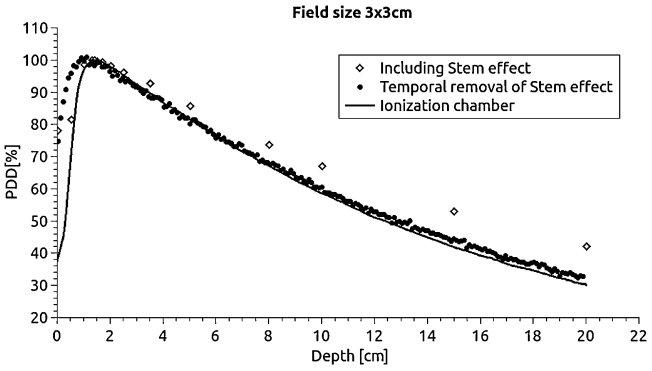

Figure 5. PPD for a window of 3 cm x 3 cm.

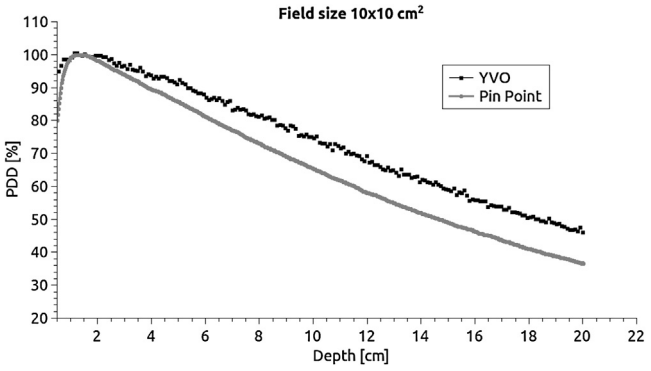

Figure 6. PPD for a window of 10 cm x 10 cm.

YVO_4:Eu^3 probe with and without the temporal filter. For comparison the signal of the pin-point ionization chamber is included.

The differences between the PDD obtained with the probe employing the temporal filtering and the pin-point chamber is owing to the higher effective Z of the YVO_4:Eu^3 with respect to the Z_{eff} of tissue. Thus, as the dimensions of a window decreases, the difference between the signal of a probe and the signal of a pin-point chamber also decreases, as shown in Figures 5, 6 and 7.

Figures 6 and 7 correspond to PDD measurements for windows of 10 cm x 10 cm and 1 cm x 1 cm respectively.

For the radiation window of 1 cm x 1 cm the PPD curve obtained with a probe coincides with the signal of a pin-point ionization chamber, except for the build-up region. This is due in part to the volume effect because the diameter of the detector is 1 mm, and the diameter of the pin-point ionization chamber is 2 mm [32]. The loss of charge particle equilibrium might also contribute to the discrepancy in the build-up region. The agreement of both PDD curves outside the build-up region means that the percentage of secondary photons having low energy is negligible compared to percentage of primary photons.

Figure 8 depicts the lateral dose profile obtained at a depth of 10 cm for a window of 3 cm x 3 cm. It is clear from the

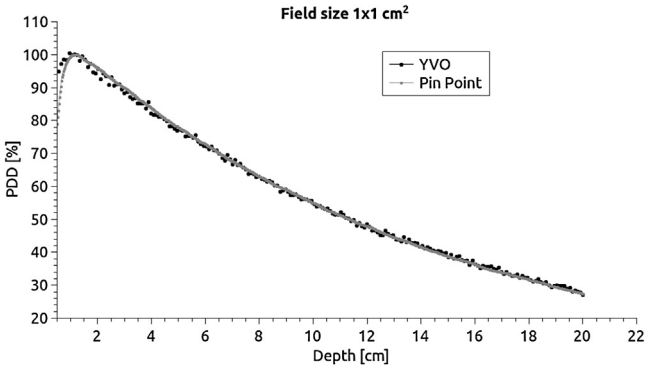

Figure 7. PDD for a window of 1 cm x 1 cm.

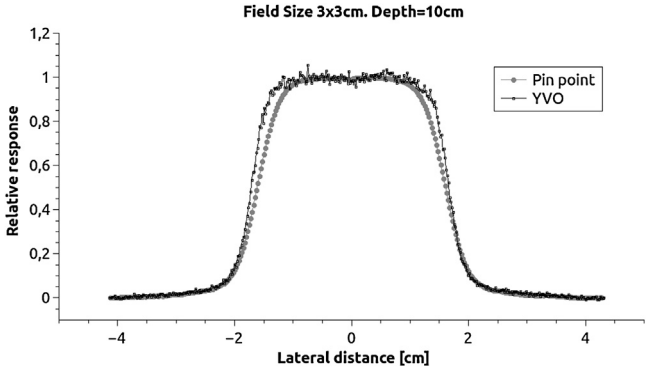

Figure 8. Lateral dose profile at a depth of 10 cm and a window of 3 cm x 3 cm.

figure that the detector has a better spatial resolution than the pin-point chamber.

Analysis of the signal decay

Figure 9 depicts the average pulse decay computed by employing 2641 pulses. It is clear that the decay is characterized by two lifetimes. The curve was fitted with the expression

$$I(t) = A1 \exp\left(-\frac{t}{t01}\right) + A2 \exp\left(-\frac{t}{t02}\right)$$

The results are t01= $1.164.10^{-5}$ s and t02= $5.38\ 10^{-4}$ s.

The fitted curve is not shown because it cannot be distinguished from the decay curve.

At this point, a remark should be made about the dose rate measurement. It can be determined, as has been done in this work, i. e., by integrating the signals delivered by the scintillator between 20 μs after a linac pulse and 2000 μ. This procedure is correct as long as the pulse repetition frequency (prf) is lower than 340 Hz since the pulses last 2.8 ms. For higher prf there is a small overlap of two consecutive RL signal. If the highest prf is, say, 400 Hz (T=2.5 ms), by integrating the RL signal between 0.3 ms and 2 ms the measured dose rate will not depend on the prf for prf's lower than 400 Hz. Another way of measuring the dose for different prf is that described in Ref. [15]. In this case the signal will depend on the prf, and the program processing the signals must include a signal correction, which will depend on the prf.

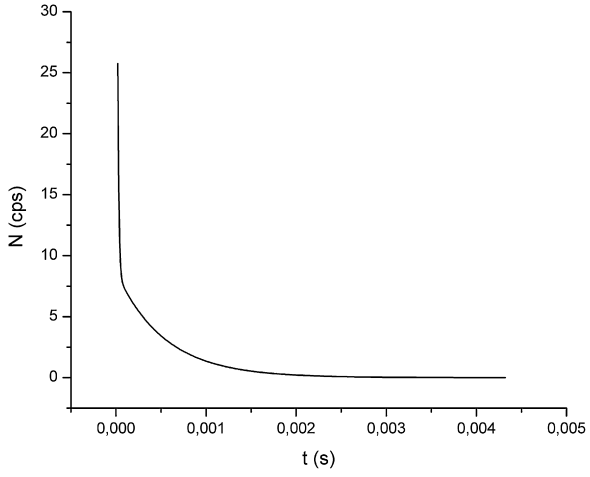

Figure 9. Average of 2641 afterglow pulses.

Temperature dependence of the signal

When used in radiotherapy the temperature of the detector might vary between 15 and 40 °C. For this reason the RL signal was measured at 15 and 40 °C in order to gain some insight into the temperature dependence of the RL signal. The water phantom was filled with water at a temperature of nearly 42 °C and let cool down. The phantom was exposed to the radiation of Theratronics machine (Co-60). At the beginning the temperature dropped at a rate of 0.05 °C /s. When the temperature reached 40 °C the phantom was irradiated during 2 minutes. The photon counting module recorded an average of 745,993 counts per second (cps). When the water reached the room temperature (15 °C) the phantom was irradiated again during 2 minutes. A rate of 747,695 cps was recorded. Thus the decrease of the signal amounts to 1.3%. This is a weaker dependence of the signal on temperature than the dependence of the signal delivered by plastic scintillators [8,9,11]. If the detector is calibrated at 28 °C, the accuracy in the measured dose is better than 1% for temperatures ranging from 15 to 40 °C.

The weak temperature dependence of the signal on temperature is a characteristic of rare earth ions [33].

Minimum detectable dose

To determine the minimum detectable dose rate the procedure described in Ref. [15] was employed. Briefly described the procedure consists in measuring the counts per second (cps) deliver by the FODdetector exposed to a Co-60 source. Measurements were carried out for different lengths of fiber, which allows finding the cps delivered by the detector for a given dose rate. The dose rate was 38.2 mGy/h, and the detector delivered 618 cps. The dark current brought about 14.5 cps ± 4.09. The lowest detection limit is given by 4 standard deviations, namely, 16.36 cps. Thus the minimum detectable dose is 1.01 mGy/h. The measurements were performed with the Hamamatsu H7421-50 photon counting head because this photon detector module features higher quantum efficiency for wavelengths longer than 600 nm than the P25PC photon counting head module.

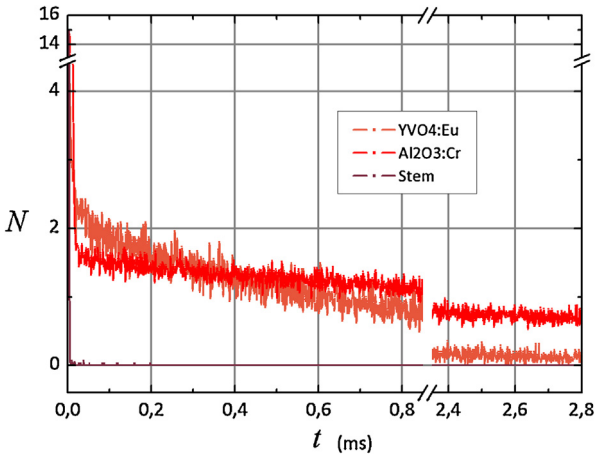

Figure 10. Comparison of the pulses delivered by YVO_4: Eu and Al_2O_3: Cr.

Comparison with the characteristics of other detectors

Some advantages of the YVO_4:Eu^{3+} compound in powder form when compared to other detectors investigated for or currently used in radiotherapy, are: 1) no previous irradiation before each measurement session is required, as is the case with both Al_2O_3:C [12], diamond detectors [34,35], and Yb3+-doped silica fibers [19], 2) lower dependence of the signal on temperature than semiconductors and PS [7–11], 4) because the afterglow of YVO4:Eu^{3+} powders lasts several milliseconds, the dose measurement employing the temporal filter is not affected by the fiber afterglow, as is the case with PS [27], and 5) a ruby rod (diameter 1 mm, length 3 mm) has a similar afterglow intensity to that of 2 mg YVO_4:Eu^{3+} powder, as shown in Figure 10. Since the active volume of the ruby rod is 2.35 mm^3, and that of the Eu doped yttrium orthovanadate is nearly 0.48 mm^3, the latter delivered a signal per volume unit nearly 5 times higher. The irradiation source was a Elekta 6 MeV and the Hamamatsu H7421-50 photon counting head was used because the quantum efficiencies for 611 nm and 694 nm are nearly equal. i. e., the emission lines of YVO4:Eu^{3+} and Al_2O_3: Cr respectively.

Finally it is worth mentioning that the response of the YVO_4:Eu^{3+} compound does not change with dose, and is stable, namely, the signal variations after repeated irradiations are less than 1%, as reported in Ref. [17].

Conclusions

The reported results indicate that the YVO_4:Eu^{3+} compound in powder form is a radioluminescent material is: 1) apt to get rid of the stem effect, and 2) suitable for dosimetry in pulsed mega-voltage photon beams, especially in modern radiotherapy, which are characterized by the superimposition of small fields, and an excellent spatial resolution is required.

Acknowledgements

The financial support by the Federal Ministry of Education and Research (Germany) and the Ministry of Science, Technology and Productive Innovation (Argentina) is gratefully acknowledged.

References

[1] Curran S, Baker W. A photoelectric alpha-particle detector. U S Atomic Energy Commision Report MDDC 1944;1296.
[2] Curran S, Baker W. A Photoelectric alpha-particle detector. Rev Sci Instruments 1948;19:116.
[3] Huang JY, Followill DS, Wang XA, Kry SF. Accuracy and sources of error of out-of field dose calculations by a commercial treatment planning system for intensity-modulated radiation therapy treatments. J Appl Clin Med Phys 2013;14:185–97.
[4] Murai T, Nakamura T, Yamamoto A. A new method of integral dose measurement with a plastic scintillator phantom. J Radiat Res 1964;5:23–35.
[5] Beddar AS, Mackie TR, Attix FH. Water-equivalent plastic scintillation detectors for high energy beam dosimetry: I. Physical characteristics and theoretical considerations. Phys Med Biol 1992;37:1883–900.
[6] Beddar AS, Mackie TR, Attix FH. Water-equivalent plastic scintillation detectors for high energy beam dosimetry: I. Properties and measurements. Phys Med Biol 1992;37:1901–13.
[7] Flühs D, Heintz M, Indenkämpen F, Wieczorek C. Direct reading measurement of absorbed dose with plastic scintillators-The general concept and applications to ophthalmic plaque dosimetry. Med Phys 1996;23:427–34.
[8] Beddar S. On possible temperature dependence of plastic scintillator response. Med Phy 2012;39:6522.
[9] Buranurak S, Andersen CE, Beierholm AR, Lindvold LR. Temperature variations as a source of uncertainty in medical fiber-coupled organic plastic scintillator dosimetry. Rad Meas 2013;56:307–11.
[10] Tanyi JA, Krafft SP, Ushino T, Huston AL, Justus BL. Performance characteristics of gated fiber-optic-coupled dosimeter in high energy pulsed photon radiation dosimetry. Appl Radiat Isotopes 2010;68:364–9.
[11] Wootton L, Beddar S. Temperature dependence of BCF plastic scintillation Detectors. Phys Med Biol 2013;58:2955–67.
[12] Andersen CE, Damkjær SMS, Kertzscher G, Greilich S, Aznar MC. Fiber-coupled radioluminescence dosimetry with saturated Al_2O_3:C crystals: Characterization in 6 and 18 MV photon beams. Rad Meas 2011;46:1090–8.
[13] Caraça Santos AM, Mohammadi M, Asp J, Monro TM, Shahraam Afshar V. Characterization of real-time fibre-coupled beryllium oxide (BeO) luminescence dosimeter in X-rar beams. Radiat Meas 2013;53-54:1–7.
[14] Jordan KJ. Evaluation of Ruby as a fluorescent sensor for fiber-based radiation dosimetry. SPIE Proceedings 1996;2705:170–8.
[15] Teichmann T, Sommer M, Henniger J. Dose rate measurements with a ruby-based optic radioluminescence probe. Rad Meas 2013;56:347–50.
[16] Pittet P, Ismail A, Ribouton J, Wnag R, Gavan JM, Chaikh A, Lu GN, Jalade P, Gireaud JY, Balosso J. Fiber background rejection and crystal overresponse compensation for GaN based in vivo dosimetry. Physica Medica 2013;29:487–92.
[17] Molina P, Santiago M, Marcazzó J, Spano F, Henniger J, Cravero W, Caselli E. Radioluminescence of red-emitting Eu-doped phosphors for fiberoptic dosimetry. Appl Radadiat Isotopes 2012;71:12–4.
[18] Molina P, Sommer M, Kattner F, Henniger J. Response characterization of an Y_2O_3:Eu-based radioluminescence probe under 60Co irradiation. Radiat Meas 2013;56:338–41.
[19] Veronese I, De Mattia C, Fasoli M, Chiodini N, Mones E, Cantone MC, Vedda A. Applied Physics Letters 2014;105:061103.
[20] Wuerfel JU. Dose measurements in small fields. Medical Physics International 1 2013;1:81–90.

[21] Mijnheer B, Beddar S, Izewska J, Reft C. In vivo dosimetry in external beam radiotherapy. Med Phys 2013;40, 070903-1 070903-19.
[22] Beddar AS, Mackie TR, Attix FH. Cerenkov light generated in optical fibres and other light pipes irradiated by electron beams. Phys Med Biol 1992;37:925–35.
[23] Lambert J, Yin Y, McKenzie DR, Law S, Suchowerska N. Cerenkov-free scintillation dosimetry in external beam radiotherapy with an air core light guide. Phys Med Biol 2008;53:3071–80.
[24] Fontbonne JM, Iltis G, Ban G, Battala A, Vernhes JC, Tillier J, Bellaize N, Le Brun C, Tamain B, Mercier K, Motin JC. Scintillating Fiber Dosimeter for Radiation Therapy Accelerator. IEEE TRANSACTIONS ON NUCLEAR SCIENCE 2002;49:2223–7.
[25] Therriault-Proulx F, Beaulieu L, Archambault L, Beddar S. On the nature of the light produced within PMMA optical light guides in scintillation fiber-optic dosimetry. Phys Med Biol 2013;58:2073–120.
[26] Liu PZY, Suchowerska N, Lambert J, Abolfathi P, McKenzie DR. Plastic scintillation dosimetry: comparison of three solutions for the Cerenkov challenge. Phys Med Biol 2011;56:5805–21.
[27] Clift MA, Johnston PN, Webb DV. A temporal method of avoiding the Cerenkov radiation generated in organic scintillator dosimeters by pulsed mega-voltage electron and photon beams. Phys Med Biol 2002;47:1421–33.
[28] Andersen CE, Marckmann CJ, Aznar MC, Botter-Jensen L, Kjaer-Kristoffersen F, Medin J. An algorithm for real time dosimetry in intensity-modulated radiation therapy using the radioluminescence signal from Al_2O_3: C. Radiat. Prot Dos 2006;120: 7–13.
[29] Beierholm AR, Lindvold LR, Andersen CE. Organic scintillators with long luminescent lifetimes for radiotherapy dosimetry. Radiat Meas 2011;46:1982–4.
[30] Beaulieu L, Goulet M, Archambault L, Beddar S. Current status of scintillation dosimetry for megavoltage beams. J of Physics: Conference Series 2013;444:012013.
[31] Weinert A. Plastic Optical Fibers (Publicis MCD Verlag) 1992.
[32] Laub WU, Wong T. The volume effect of detectors in the dosimetry of small fields used in IMRT. Med Phys 2003;30:341–7.
[33] Phosphor Handbook, edited by S. Shionoya and W. M. Yen, CRC Press 1998.
[34] Westermark M, Arndt J, Nilsson B, Brahme A. Comparative dosimetry in narrow high-energy photons beams. Phys Med Biol 2000;45:685–702.
[35] According to the specifications of the microDiamond detector type 60019, PTW, Germany, a pre-irradiation dose of 5 Gy is necessary previous to the use of the detector.

Available online at www.sciencedirect.com
ScienceDirect